



Research paper

Kinetics of the E46Q mutant of photoactive yellow protein investigated by transient grating spectroscopy

Cheolhee Yang^{a,b,1}, Tae Wu Kim^{a,b,1}, Youngmin Kim^b, Jungkweon Choi^b, Sang Jin Lee^{a,b}, Hyotcherl Ihee^{a,b,*}^a Department of Chemistry, Korea Advanced Institute of Science and Technology (KAIST), Daejeon 34141, Republic of Korea^b Center for Nanomaterials and Chemical Reactions, Institute for Basic Science (IBS), Daejeon 34047, Republic of Korea

ARTICLE INFO

Article history:

Received 11 January 2017

In final form 7 March 2017

Available online 8 March 2017

Keywords:

Photoactive yellow protein

Transient grating spectroscopy

Diffusion coefficient

ABSTRACT

To elucidate the role of internal proton transfer in the photodynamics of photoactive yellow protein (PYP), the photocycle of the Glu46Gln mutant of PYP (E46Q-PYP) is investigated by transient grating (TG) spectroscopy. Compared with wild-type PYP (wt-PYP), the first spectrally blue-shifted intermediate of E46Q-PYP is formed more slowly, which is consistent with the absence of direct protonation from Glu46 residue, if the parallel kinetic model for wt-PYP is invoked. The smaller conformational change in E46Q-PYP, as manifested by the smaller change in the diffusion coefficient, mainly arises from the relatively larger volume of the ground state E46Q-PYP than wt-PYP rather than from the smaller volume of the pB state.

© 2017 Elsevier B.V. All rights reserved.

1. Introduction

Photoactive yellow protein (PYP) is a globular protein expressed in the halophilic purple bacterium *Halorhodospira halophila*. PYP has been extensively investigated as a model system for photoreceptor proteins. Upon blue light illumination, PYP undergoes a photocyclic reaction triggered by the *trans-cis* isomerization of the chromophore, *p*-coumaric acid (*p*CA), and participates in signal transduction processes [1–7]. After excitation by blue light, ground state PYP (pG; $\lambda_{\text{max}} = 446$ nm) is converted to spectrally red-shifted intermediates (pR; $\lambda_{\text{max}} = 465$ nm) via an increase in the negative charge on the phenolic oxygen of the chromophore. Sequentially, the red-shifted intermediates are transformed into spectrally blue-shifted intermediates (pB; $\lambda_{\text{max}} = 355$ nm). During the formation of blue-shifted intermediates, the hydrogen bonds between *p*CA and neighboring amino acids (Tyr42 and Glu46) are broken and *p*CA is then protonated by internal proton transfer from Glu46 [2,8–10]. This internal proton transfer from Glu46 to *p*CA is believed to be an important step in the expression of the putative signaling state during the photocycle of PYP [2,4,6,9–14]. Two kinetic models have been proposed for the photoreaction of wild-type PYP (wt-PYP) (Fig. 1(a) and (b)). The sequential kinetic model has been more frequently used in the literature [10,15–18], but an

alternative model including parallel pathways from two pR species (pR_{E46Q} and pR_{CW}) to the first pB species (pB₁) was also proposed [2,8,11]. The parallel kinetics with the bifurcated transitions is based on the coexistence of two pR species in the sub-microsecond and microsecond time regime determined from time-resolved Laue crystallography [2,19,20] and the much weaker TA signal for the transition from pR₁ to pB₁ [17]. Specifically, pR_{E46Q} (or pR₁) only retains the hydrogen bond between the chromophore and Tyr42, while pR_{CW} (or pR₂) involves two hydrogen bonds to Tyr42 and Glu46 [2,19,20] (Fig. 1(a)).

To elucidate the role of the 46th residue in the PYP photocycle, the E46Q-PYP mutant, in which Glu46 is substituted with Gln, has been employed. During the photocycle of E46Q-PYP, internal proton transfer from the 46th residue to *p*CA is inhibited due to the weakness of hydrogen bond between Gln46 and *p*CA [10,19,21–24]. The X-ray crystallographic study showed that the distance of hydrogen bond from 46th residue to the phenolate oxygen of *p*CA in E46Q-PYP was longer than that in wt-PYP, linked to the weakness of hydrogen bond network [25]. The time-resolved Laue crystallographic studies revealed that the two types of pR-like intermediates, termed IE1 and IE2, have chromophore structures and hydrogen bond networks similar with those in pR₁ of wt-PYP (Fig. 1(c)) [26]. To probe the protein conformational dynamics in solution, the various studies employing the experimental techniques with the structural sensitivity, such as FT-IR [10], time-resolved X-ray solution scattering (TRXSS) [21], and NMR [22], have demonstrated that the formation of blue-shifted intermediates in E46Q-PYP includes smaller conformational changes than

* Corresponding author at: Department of Chemistry, Korea Advanced Institute of Science and Technology (KAIST), Daejeon 34141, Republic of Korea.

E-mail address: hyotcherl.ihee@kaist.ac.kr (H. Ihee).

¹ These authors are contributed equally to this work.

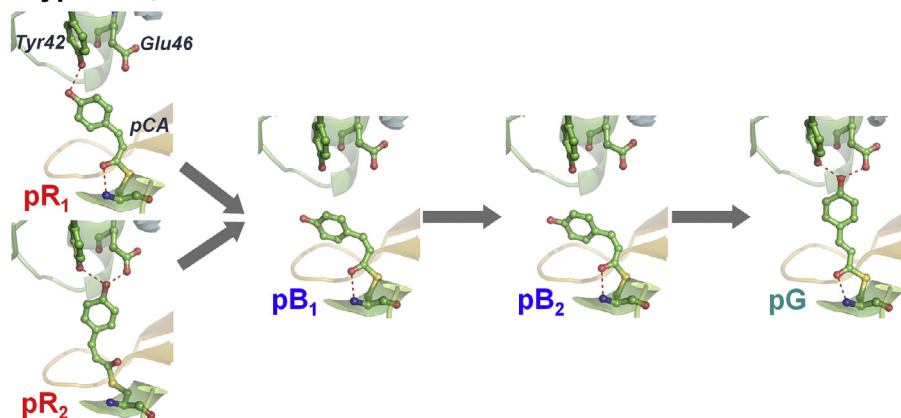
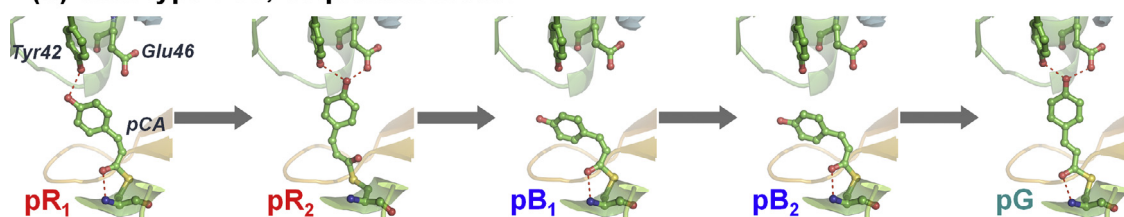
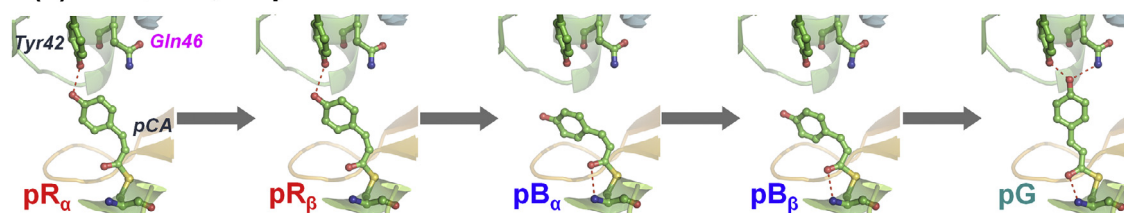
(a) Wild-type PYP, Parallel model**(b) Wild-type PYP, Sequential model****(c) E46Q-PYP, Sequential model**

Fig. 1. Kinetic models of PYP reflecting chromophore structural change. (a) Parallel kinetic model of wild-type PYP (wt-PYP), determined by time-resolved X-ray Laue crystallography (TR-Laue) [2], together with the chromophore structure and its hydrogen bonds to the neighboring residues. In solution, the two pR intermediates of pR₁ and pR₂, determined by time-resolved X-ray solution scattering (TRXSS) [11], are matched with pR_{E46Q} and pR_{CW} in crystalline phase, respectively. The coexistent two pR intermediates undergo the bifurcated transition toward pB₁. (b) Sequential kinetic model of wt-PYP conventionally used in the literatures [10,15–18]. The chromophore structures of two pR intermediates determined from TR-Laue [2] are reorganized in order of occurrence of intermediates. (c) Sequential kinetic model of E46Q-PYP determined by TRXSS [21] and TR-Laue [26]. In solution, the intermediates of pR_α, pR_β, pB_α, and pB_β, determined by TRXSS, are linked to IE1, IE2, IL1, and IL2 in crystalline phase, respectively. Comparing the intermediates of E46Q-PYP with those of wt-PYP, the chromophore structure of pR₂-like intermediate in wt-PYP is absent in E46Q-PYP.

that in wt-PYP. In particular, the TRXSS measurement showed that the photocycle of E46Q-PYP follows the sequential kinetics, unlike the case of wt-PYP where the parallel kinetics was proposed to be more appropriate than the sequential kinetics [21]. In addition, transient absorption (TA) spectroscopic studies have been performed to investigate the electronic state related with chromophore and its surrounding environment [4,7,8,21,27–30]. TA results showed the apparently faster rates in E46Q-PYP than in wt-PYP, which were interpreted to indicate that pR (or I₁) intermediate and pB (or I₂) intermediate in E46Q-PYP are rapidly formed relative to in wt-PYP. Based on the TA studies, it was suggested that the altered kinetics in E46Q-PYP might be due to lack or weakness of the hydrogen bond between 46th residue and pCA [8,27]. Despite the various kinetic studies for the photoreaction of E46Q-PYP, the role of 46th residue during the photocycle is still not comprehended.

In this study, using the transient grating (TG) technique, we investigated the role of the 46th residue in the PYP photocycle in terms of global protein conformational changes. To do so, the E46Q-PYP mutant was employed and its dynamics was compared with that of wt-PYP. TG spectroscopy can detect changes in the dif-

fusion coefficient, which is directly related to the molecular volume and size of a protein [12,31,32]. Thus, TG spectroscopy is complementary to other time-resolved techniques, such as TRXSS, TA, and time-resolved vibrational spectroscopies. The results presented in this study confirm that the apparent rate constant in the transition from pR to pB in E46Q-PYP is significantly accelerated compared with that in wt-PYP, consistent with TA studies [8,21,30]. However, if the parallel kinetics for wt-PYP is considered as shown in Fig. 1(a), the formation of pB species is actually decelerated in the E46Q mutant compared with wt-PYP. This may resolve the long-standing puzzle of why the rate appears to be accelerated for E46Q-PYP even if the direct protonation from the 46th residue is inhibited. The TG results show that the difference between the diffusion coefficients of the pB and pG states (ΔD) in E46Q-PYP is smaller than that in wt-PYP, confirming that conformational changes are restricted in the signaling process of E46Q-PYP. Importantly, the smaller ΔD in E46Q-PYP is mainly due to the smaller diffusion coefficient of the pG state (D_{pG}) in E46Q-PYP compared with that in wt-PYP. This indicates that the smaller conformational change in E46Q-PYP is related to the larger volume of the pG state in E46Q-PYP than in wt-PYP rather than the smaller volume of the pB state.

2. Methods

2.1. Preparation of the E46Q mutant PYP

A protein sample was prepared as described previously [21]. Briefly, the gene encoding E46Q-PYP was introduced into the pQE80L vector and expressed in *Escherichia coli* BL21 (DE3). The expressed apo-E46Q-PYP was reconstituted with *p*-coumaric anhydride. The holo-E46Q-PYP was purified by centrifugation and Ni-affinity chromatography. After buffer exchange, the extra sequence at the N-terminus of the protein was removed by overnight treatment with enterokinase. The protein solution was purified again by ion exchange chromatography and dialyzed with the buffer used for the TG experiments (20 mM sodium phosphate and 20 mM NaCl, pH 7.0). The purity index of E46Q-PYP ($Abs_{280\text{ nm}}/Abs_{460\text{ nm}}$) was 0.43. The sample solution of wt-PYP in the same buffer conditions was prepared in the same way as that of E46Q-PYP. The purity index of wt-PYP ($Abs_{280\text{ nm}}/Abs_{446\text{ nm}}$) was 0.45.

2.2. TG spectroscopy

The TG experiment was performed as described elsewhere [31,32]. Briefly, 380 μM E46Q-PYP dissolved in the buffer solution described above was added to a quartz cell (2 mm path length). An optical parametric oscillator (LOTIS) pumped by a third harmonic of a Nd:YAG laser (EKSPILA; pulse width <6 ns) generated pump pulses (460 nm, 0.5 Hz). The pump beam was split into two identical beams. The fluence of each pump beam at the sample position was 9.5 $\mu\text{J}/\text{mm}^2$. A diode laser (Thorlabs; 830 nm, continuous wave) was used as the probe beam. The power of the probe beam was adjusted to be as weak as possible to prevent photodegradation of the protein. Since the probe light was nonresonant with either the ground or the intermediate state of E46Q-PYP, the TG signal reflects only the transient change in the refractive index, rather than the transient absorption change. The two pump beams and the probe beam were focused onto the same spot on the sample cell. The probe beam diffracted by the transient grating was filtered by using a long-pass filter to remove the scattered pump pulse and was detected using a photomultiplier tube (Hamamatsu) and an oscilloscope (Tektronix). For every measurement, 160 TG signals were averaged to improve the signal-to-noise ratio. To acquire data at various grating wavenumbers (q), TG signals at various angles of the two pump beams were measured. TG signals for wt-PYP under the same buffer conditions were measured in the same way as signals for E46Q-PYP. An aqueous bromocresol purple (BCP) solution was used as a thermal reference sample. Because BCP releases the excitation energy only as heat, the TG signal of the BCP solution arises from only the thermal diffusion, allowing us to determine the q values. All TG measurements were implemented at room temperature (293 K).

3. Results and discussion

To investigate the effects of site-directed mutagenesis on the photocycle of PYP, we measured TG signals for E46Q-PYP and wt-PYP. To accurately determine the diffusion coefficients of the reactant and photoproduct involved in the photocycle, we measured TG signals with various q values, which are determined by the angle between the propagation directions of two pump beams. Fig. 2 shows the TG signals for both E46Q-PYP and wt-PYP measured at various q values. The shapes of the TG signals for both E46Q-PYP and wt-PYP measured in this study are similar to those for wt-PYP reported in previous TG studies [12,18,33–35]. First, a very small rise component is observed in the sub-microsecond region, followed by a significant decay process. Subsequently,

two sets of rise and decay appear in the time region from tens of microseconds to hundreds of milliseconds. For both E46Q-PYP and wt-PYP, we simultaneously fitted the TG signals at the five q values according to the following function of the square of an exponential series:

$$I_{TG}(t) = \alpha \left\{ \begin{array}{l} \delta n_1 \exp\left(-\frac{t}{\tau_1}\right) + \delta n_{th} \exp(-D_{th}q^2t) \\ + \delta n_2 \exp\left(-\frac{t}{\tau_2}\right) + \delta n_3 \exp\left(-\frac{t}{\tau_3}\right) \\ + \delta n_4 \exp\left(-\frac{t}{\tau_4}\right) + \delta n_5 \exp\left(-\frac{t}{\tau_5}\right) \end{array} \right\}^2$$

where α is a constant, δn_1 , δn_2 , δn_3 , δn_4 , and δn_5 are the refractive index changes, τ_1 , τ_2 , τ_3 , τ_4 , and τ_5 are the time constants for the corresponding processes, and δn_{th} and D_{th} are the refractive index change and diffusivity, respectively, induced by the thermal effect. In the global fitting of the TG signals, τ_1 , τ_2 , and τ_3 , which are independent of the q value, are the time constants for the photoreaction of PYP. These three time constants were used as the global parameters of the TG signals at the five different q values. The τ_4 and τ_5 values, the time constants for the diffusion of proteins, depend on the q value, and thus were individually determined for each TG signal. As depicted in Fig. 2, the reconstructed theoretical TG signals for E46Q-PYP and wt-PYP are in good agreement with the corresponding experimental data. Considering the principle of TG spectroscopy [12,18,31–35], the diffusion rate constants of k_4 and k_5 , which are $1/\tau_4$ and $1/\tau_5$, respectively, can be expressed as $k_4 = D_4 \times q^2$ and $k_5 = D_5 \times q^2$. The diffusion coefficients of proteins, D_4 and D_5 , were determined from the slope of the plot of the rate constants of k_4 and k_5 against q^2 (Fig. 3). Based on previous TG studies for PYP [12,18,33–35], protein species responsible for D_4 and D_5 can be assigned as follows. The refractive index changes of δn_4 and δn_5 for both E46Q-PYP and wt-PYP determined from TG signals have negative and positive signs, respectively. The opposite signs in the refractive index changes can be explained by the phase difference of 180° for the spatial modulation between the reactant and product. In this regard, the diffusion coefficients of D_4 and D_5 for both E46Q-PYP and wt-PYP are linked to the reactant and the product, respectively. In the photocycle of PYP, the ground state, the pR-like intermediates, and the pB-like intermediates can contribute to the molecular diffusion process. First, it is obvious that the diffusion coefficient of the reactant, D_4 , corresponds to the diffusion coefficient of pG (D_{pG}). The diffusion coefficients for the pR-like intermediates would not be detectable because the decay time constants for the pR-like intermediates (in sub-millisecond) are much faster than the time constant for the molecular diffusion. The molecular diffusion process of pB-like intermediates should be detectable due to relatively long lifetimes, and thus D_5 can be linked to the diffusions of the pB-like intermediates (D_{pB}). In the previous TG studies for wt-PYP [12,18,33–35], it was reported that the two diffusion coefficients can describe the TG signals, and one of them was assigned to the diffusion coefficient for two pB-like intermediates. Considering the consistency with the previous TG results in view of the number of diffusion coefficients, D_{pB} in E46Q-PYP corresponds to the diffusion coefficient of two pB intermediates, which is in line with D_{pB} in wt-PYP.

It should be noted that the kinetics for the photocycle of E46Q-PYP is different from that of wt-PYP. Furthermore, the structures of the intermediates formed during the photocycle of E46Q-PYP are not identical to those of the intermediates observed for wt-PYP, which are supported by the previous studies [21,26]. For this reason, the four intermediates formed during the photocycle of E46Q-PYP are designated differently from those of wt-PYP as pR $_{\alpha}$, pR $_{\beta}$, pB $_{\alpha}$, and pB $_{\beta}$ [21]. From the quantitative analysis of TG signals for E46Q-PYP, three time constants were determined: $3.0 \pm 0.6 \mu\text{s}$, $85 \pm 5 \mu\text{s}$, and $2.7 \pm 4.1 \text{ ms}$, respectively. From the plot

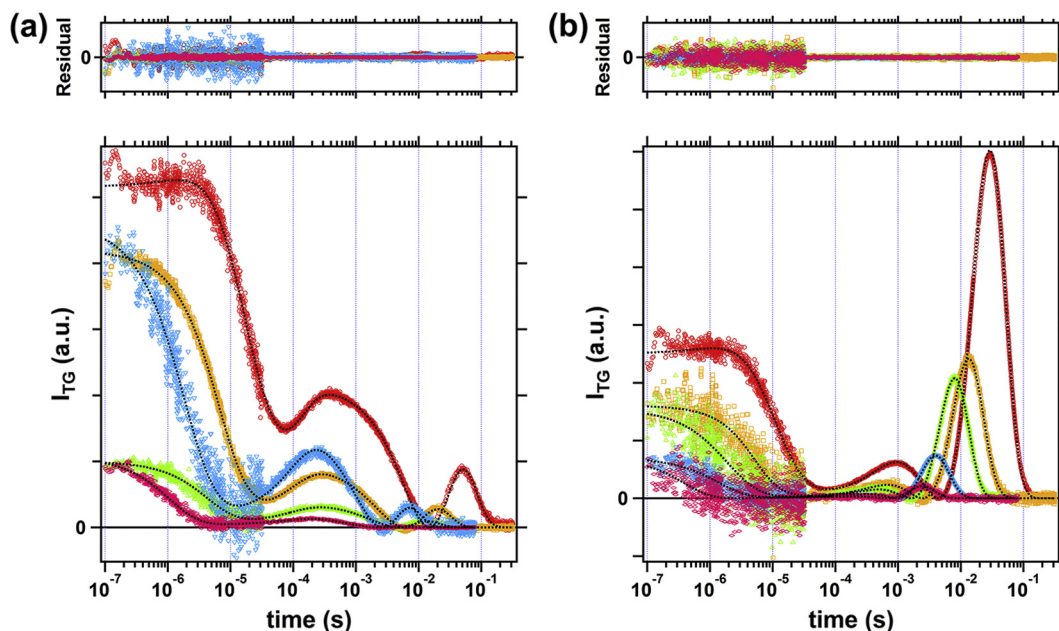


Fig. 2. Fitting results of transient grating signals of E46Q-PYP and wt-PYP. Temporal profiles of the transient grating signals of (a) E46Q-PYP and (b) wt-PYP are shown. The q^2 values for the signals for E46Q-PYP were $0.27 \times 10^{12} \text{ m}^{-2}$ (red), $0.71 \times 10^{12} \text{ m}^{-2}$ (orange), $1.21 \times 10^{12} \text{ m}^{-2}$ (green), $2.55 \times 10^{12} \text{ m}^{-2}$ (cyan), and $3.28 \times 10^{12} \text{ m}^{-2}$ (magenta), and those for the signals for wt-PYP were $0.37 \times 10^{12} \text{ m}^{-2}$ (red), $0.91 \times 10^{12} \text{ m}^{-2}$ (orange), $1.63 \times 10^{12} \text{ m}^{-2}$ (green), $3.67 \times 10^{12} \text{ m}^{-2}$ (cyan), and $6.61 \times 10^{12} \text{ m}^{-2}$ (magenta). The black dotted lines are the fits from the simultaneous fitting analyses. The residuals of the fits shown in the top panel demonstrate the high fitting quality. (For interpretation of the references to colour in this figure legend, the reader is referred to the web version of this article.)

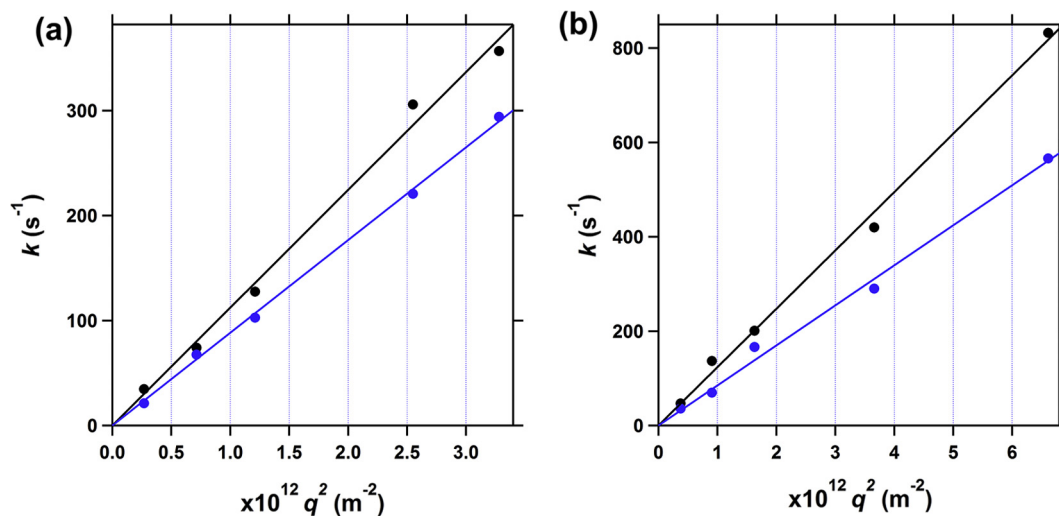


Fig. 3. Plots of diffusion rates against the square of grating wavenumbers. Two rate constants k_4 (black) and k_5 (blue) for (a) E46Q-PYP and (b) wt-PYP are plotted against q^2 values. k_4 and k_5 , determined by fitting the TG signals at each q value, are shown as solid circles. Both k_4 and k_5 were well-fitted by a linear line equation with zero y-intercepts (solid lines). (For interpretation of the references to colour in this figure legend, the reader is referred to the web version of this article.)

of the rate constants k_4 and k_5 against q^2 (Fig. 3(a)), D_{pG} and D_{pB} of E46Q-PYP were determined to be $(1.12 \pm 0.03) \times 10^{-10} \text{ m}^2 \text{ s}^{-1}$ and $(0.88 \pm 0.01) \times 10^{-10} \text{ m}^2 \text{ s}^{-1}$, respectively. Based on the results obtained from a previous study [21], we assign three time constants for E46Q-PYP to the transitions from pR_α to pR_β , from pR_β to pB_α , and from pB_α to pB_β , respectively (Fig. 4(a)). In the case of wt-PYP, three time constants of $1.9 \pm 0.2 \mu\text{s}$, $480 \pm 20 \mu\text{s}$, and $2.7 \pm 0.6 \text{ ms}$ were determined and assigned to the decay process of pR_1 , the transition from pR_2 to pB_1 , and the transition from pB_1 to pB_2 , respectively (Fig. 4(b) and (c)). Additionally, D_{pG} and D_{pB} of wt-PYP were determined to be $(1.24 \pm 0.03) \times 10^{-10} \text{ m}^2 \text{ s}^{-1}$ and $(0.85 \pm 0.02) \times 10^{-10} \text{ m}^2 \text{ s}^{-1}$, respectively (Fig. 3(b)). For both E46Q-PYP and wt-PYP, the pB to pG recovery is irrelevant to the TG signal because diffusion of the protein occurred on a much fas-

ter time scale than the ground state recovery (usually several hundreds of milliseconds for wt-PYP).

Comparing the time constants for E46Q-PYP with those for wt-PYP indicates that the rate in the transition from pR -like intermediates to pB -like intermediates is accelerated in E46Q-PYP, which is consistent with the results from TA spectroscopy [8,21,30]. According to the comparative TA study of wt-PYP and E46Q-PYP, the absorption spectra of 1st pB intermediate of E46Q-PYP (pB_α) and that of wt-PYP (pB_1) are similar but not identical [8]. However, in view of chromophore structure and its surrounding environment, the transitions to the 1st pB intermediates for E46Q-PYP and wt-PYP are comparable to each other since they accompany similar conformational changes associated with the disruption of the hydrogen bond network and the protonation of the chro-

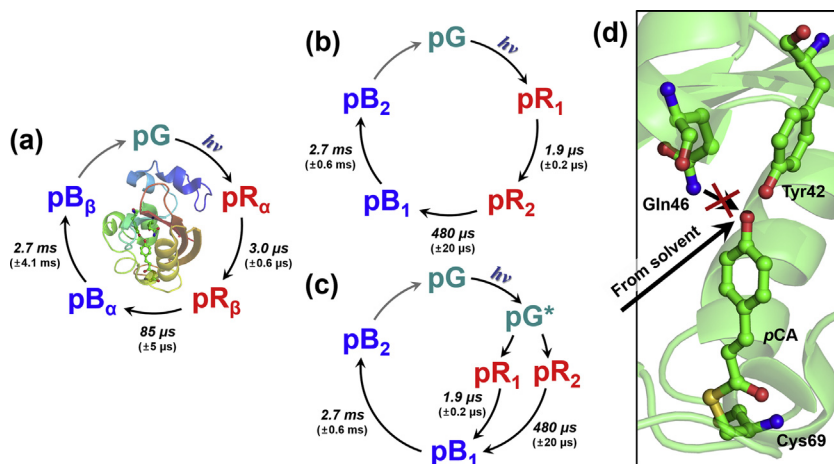


Fig. 4. Photocycles and structure of E46Q-PYP. (a) Photocycle of E46Q-PYP is shown. Ground state (pG) and four intermediates (pR_α, pR_β, pB_α, and pB_β) of E46Q-PYP are shown with the time constants determined by transient grating spectroscopy. The structure of E46Q-PYP is visualized in the center of the photocycle of E46Q-PYP (PDB ID: 1OTA). For clarity, the protein backbone and the active site around the chromophore are shown as ribbon and ball-and-stick models, respectively. (b and c) Schemes of the sequential model (b) and parallel model (c) for the photocycle of wt-PYP are shown. pG and four intermediates (pR₁, pR₂, pB₁, and pB₂) are shown with the time constants determined by transient grating spectroscopy. (d) The chromophore (pCA) and the adjacent residues (Tyr42, Gln46, and Cys69) nearby the chromophore of E46Q-PYP are shown (PDB ID: 1OTA). Possible routes for the protonation of pCA are shown (arrows). The internal proton transfer from the 46th residue, which is responsible for the protonation of the chromophore in wt-PYP, is inhibited in E46Q-PYP, whereas the proton uptake from the bulk aqueous phase is not blocked.

mophore. The most prominent effect by the mutation of the 46th residue in E46Q-PYP is observed in τ_2 (85 μ s) for the formation of pB_α, which can be compared with τ_2 in wt-PYP (480 μ s), whereas the other two time constants are similar to each other. In addition, during the photoreaction of wt-PYP, the pR intermediates are mainly protonated by the internal proton transfer from Glu46 [10], although the external proton transfer from the bulk aqueous phase cannot be ruled out [28,36]. From this point of view, it is expected that the mutation of Glu46 into Gln significantly slows down the transition from pR to pB due to the absence of internal proton transfer from the 46th residue, as shown in Fig. 4 (d). Based on the previous studies, there are two proposed kinetic models for wt-PYP, which are the sequential kinetic model [15,16] and the parallel kinetic model [2,8,11]. In the framework of the sequential kinetic model for wt-PYP (Fig. 4(b)), the formation of early pB species (pB₁ for wt-PYP and pB_α for E46Q-PYP) appears much faster in E46Q-PYP (85 μ s) than in wt-PYP (480 μ s). This runs counter to the expected deceleration of the protonation process in E46Q-PYP due to the inhibited direct protonation from the 46th residue. By contrast, in the framework of the parallel kinetic model for wt-PYP (Fig. 4(c)), pB species can be directly formed from pR₁, and thus the formation of pB_α for E46Q-PYP should be compared with the transition from pR₁ to pB₁ for wt-PYP. In this case, the formation of pB_α for E46Q-PYP (85 μ s) is significantly slower than the transition from pR₁ to pB₁ for wt-PYP (1.9 μ s), and the deceleration of the pB formation in E46Q-PYP can be explained by the absence of internal proton transfer from the 46th residue.

According to previous TG studies of wt-PYP, D_{pG} and D_{pB} of wt-PYP are in the ranges of $(1.4\text{--}1.2) \times 10^{-10} \text{ m}^2 \text{ s}^{-1}$ and $(1.2\text{--}1.0) \times 10^{-10} \text{ m}^2 \text{ s}^{-1}$, respectively [12,18,33–35]. The D_{pB} value of wt-PYP determined in this study ($0.85 \times 10^{-10} \text{ m}^2 \text{ s}^{-1}$) is smaller than those reported in previous studies, whereas D_{pG} of wt-PYP is similar to those reported in previous studies [12,18,33–35]. Since the buffer solution used in previous TG studies of wt-PYP (10 mM Tris-HCl with 1 mM phenylmethanesulfonyl fluoride, pH 8.0) [12,18,33–35] is quite different from that used in this study (20 mM sodium phosphate with 20 mM NaCl, pH 7.0), the smaller D_{pB} of wt-PYP in this study may be explained by the different solution environment.

Notably, D_{pG} of E46Q-PYP ($1.12 \times 10^{-10} \text{ m}^2 \text{ s}^{-1}$) is significantly smaller than D_{pG} of wt-PYP ($1.24 \times 10^{-10} \text{ m}^2 \text{ s}^{-1}$). According to

the Stokes-Einstein relationship, $D = k_B T / 6\pi\eta r$ (where D is the molecular diffusion coefficient, k_B is the Boltzmann constant, T is the temperature, η is the viscosity of the solution, and r is the Stokes radius), this result indicates that E46Q-PYP has a larger hydrodynamic radius (and possibly a larger volume) than that of wt-PYP. Kim et al. showed that the R_g value of the pG state of E46Q-PYP reported by TRXSS (15.10 Å) is larger than that of wt-PYP (14.83 Å) [21], indicating that the volume of E46Q-PYP is larger than that of wt-PYP. Interestingly, D_{pB} of E46Q-PYP ($0.88 \times 10^{-10} \text{ m}^2 \text{ s}^{-1}$) is only slightly larger than that of wt-PYP ($0.85 \times 10^{-10} \text{ m}^2 \text{ s}^{-1}$). This implies that the pB state of E46Q-PYP has a slightly more compact structure compared with that of wt-PYP. Because a single D_{pB} value is used for two pB intermediates, an average of R_g values for two pB intermediates can be taken for the comparison with the corresponding D_{pB} . Based on the results from TRXSS, the average R_g value for two pB intermediates of E46Q-PYP is 15.34 Å and that of wt-PYP is 15.47 Å [21]. The difference in the average R_g values between E46Q-PYP and wt-PYP is 0.13 Å for pB, which is smaller than the value for pG (0.27 Å). This trend is consistent with the smaller change in the diffusion coefficients between E46Q-PYP and wt-PYP for pB ($\Delta D_{pB} = 0.03 \times 10^{-10} \text{ m}^2 \text{ s}^{-1}$) than that for pG ($\Delta D_{pG} = 0.12 \times 10^{-10} \text{ m}^2 \text{ s}^{-1}$).

As the difference between D_{pG} and D_{pB} (ΔD) in E46Q-PYP ($0.24 \times 10^{-10} \text{ m}^2 \text{ s}^{-1}$) is smaller than that in wt-PYP ($0.39 \times 10^{-10} \text{ m}^2 \text{ s}^{-1}$), the TG results confirm that the global conformational change between pB and pG states for E46Q-PYP is smaller than that for wt-PYP, which is consistent with the previous results. An FT-IR study on E46Q-PYP reported that during pB formation, the extent of amide-I band absorption in the antiparallel β -structure of E46Q-PYP is smaller than that of wt-PYP, and a band for the ND-containing side chain group (Arg, Asn, or Gln) of wt-PYP is not present in the case of E46Q-PYP [10]. An NMR study of E46Q-PYP by Derix et al. demonstrated that, in contrast to wt-PYP, the pB state of E46Q-PYP shows relatively intense HSQC peaks corresponding to the N-terminal region, indicating the N-terminal region of E46Q-PYP exhibits smaller conformational changes than that of wt-PYP [22]. The shape reconstruction from the TRXSS signal also showed that E46Q-PYP undergoes smaller structural changes than that of wt-PYP during the formation of blue-shifted intermediates [21].

Since the difference between D_{pG} values of E46Q-PYP and wt-PYP ($0.12 \times 10^{-10} \text{ m}^2 \text{ s}^{-1}$) is much larger than the difference

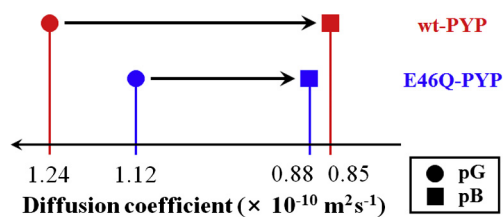


Fig. 5. Schematic representation of the changes in diffusion coefficients for E46Q-PYP and wt-PYP. The ground (pG) and blue-shifted intermediate (pB) states of E46Q-PYP (blue) and wt-PYP (red) are shown as circles and squares, respectively. The diffusion coefficients of the ground state (D_{pG}) and the blue-shifted intermediate (D_{pB}) are indicated below the line. (For interpretation of the references to colour in this figure legend, the reader is referred to the web version of this article.)

between D_{pB} values ($0.03 \times 10^{-10} \text{ m}^2 \text{ s}^{-1}$), as schematically shown in Fig. 5, the smaller conformational change of E46Q-PYP than wt-PYP is mainly attributed to the larger volume of the pG state of E46Q-PYP compared with that of wt-PYP. In an NMR study, Derix et al. suggested that the structure of the pG state of E46Q-PYP strongly resembles that of wt-PYP [22]. However, chemical shifts in E46Q-PYP and wt-PYP were not identical in that study, indicating that the local structure of E46Q-PYP could be slightly different from that of wt-PYP. The pG state of E46Q-PYP may exhibit a more globally swollen conformation than that of wt-PYP, as described in this study, whereas the local conformation of the pG states of E46Q-PYP and wt-PYP may be only slightly different owing to the different global conformations of the proteins. Thus, the larger volume of the pG state of E46Q-PYP relative to that of wt-PYP, as determined in this study, does not contradict the NMR results. It should be noted that the buffer conditions in the NMR study and in this work are not the same. Unlike TRXSS [21], which was performed using the same buffer environment used in this study, the results of the NMR study [22] are not directly comparable with our TG results owing to different buffer conditions. In this context, a detailed investigation of the PYP photocycle and conformational change depending on the buffer composition is needed to fully elucidate the conformational changes in PYP.

4. Conclusions

In this study, the photocycle of E46Q-PYP was investigated by TG spectroscopy. A comparison of the kinetics of E46Q-PYP and wt-PYP shows an apparent acceleration of the formation of the early blue-shifted intermediate in E46Q-PYP, which is consistent with TA studies [8,21,30]. The formation of the early blue-shifted intermediate appears to be accelerated in E46Q-PYP if the sequential kinetics is operational for the photocycle of wt-PYP, and such acceleration is not consistent with the expected deceleration of the protonation process due to the absence of internal proton transfer from the 46th residue in E46Q-PYP. The parallel kinetics for wt-PYP, where the first blue-shifted intermediate can be directly formed from pR₁, resolves this inconsistency. In addition to the kinetics, the diffusion coefficients measured by TG signals confirm the smaller global conformational change accompanied by the formation of the blue-shifted intermediate in E46Q-PYP than in wt-PYP. Interestingly, the smaller change from D_{pG} to D_{pB} in E46Q-PYP compared with wt-PYP is mainly caused by the larger difference between E46Q-PYP and wt-PYP in D_{pG} than that in D_{pB} (Fig. 5).

Acknowledgments

This work was supported by IBS-R004-A1.

References

- [1] L. Ujj, S. Devanathan, T.E. Meyer, M.A. Cusanovich, G. Tollin, G.H. Atkinson, *Biophys. J.* 75 (1998) 406.
- [2] H. Ihee, S. Rajagopal, V. Srajer, R. Pahl, S. Anderson, M. Schmidt, F. Schotte, P.A. Anfinrud, M. Wulff, K. Moffat, *Proc. Natl. Acad. Sci. USA* 102 (2005) 7145.
- [3] L.J.G.W. van Wilderen, M.A. van der Horst, I.H.M. van Stokkum, K.J. Hellingwerf, R. van Grondelle, M.L. Groot, *Proc. Natl. Acad. Sci. USA* 103 (2006) 15050.
- [4] Y. Zhou, L. Ujj, T.E. Meyer, M.A. Cusanovich, G.H. Atkinson, *J. Phys. Chem. A* 105 (2001) 5719.
- [5] K. Pande, C.D.M. Hutchison, G. Groenhof, A. Aquila, J.S. Robinson, J. Tenboer, S. Basu, S. Boutet, D.P. DePonte, M.N. Liang, T.A. White, N.A. Zatsepin, O. Yefanov, D. Morozov, D. Oberthuer, C. Gati, G. Subramanian, D. James, Y. Zhao, J. Koralek, J. Brayshaw, C. Kupitz, C. Conrad, S. Roy-Chowdhury, J.D. Coe, M. Metz, P.L. Xavier, T.D. Grant, J.E. Koglin, G. Ketawala, R. Fromme, V. Srajer, R. Henning, J.C.H. Spence, A. Ourmazd, P. Schwander, U. Weierstall, M. Frank, P. Fromme, A. Barty, H.N. Chapman, K. Moffat, J.J. van Thor, M. Schmidt, *Science* 352 (2016) 725.
- [6] R. Brudler, R. Rammelsberg, T.T. Woo, E.D. Getzoff, K. Gerwert, *Nat. Struct. Biol.* 8 (2001) 265.
- [7] P. Changenet-Barret, P. Plaza, M.M. Martin, H. Chosrowjan, S. Taniguchi, N. Mataga, Y. Imamoto, M. Kataoka, *J. Phys. Chem. C* 113 (2009) 11605.
- [8] S. Yermenko, I.H.M. van Stokkum, K. Moffat, K.J. Hellingwerf, *Biophys. J.* 90 (2006) 4224.
- [9] K.J. Hellingwerf, J. Hendriks, T. Gensch, *J. Phys. Chem. A* 107 (2003) 1082.
- [10] A.H. Xie, L. Kelemen, J. Hendriks, B.J. White, K.J. Hellingwerf, W.D. Hoff, *Biochemistry* 40 (2001) 1510.
- [11] T.W. Kim, J.H. Lee, J. Choi, K.H. Kim, L.J. van Wilderen, L. Guerin, Y. Kim, Y.O. Jung, C. Yang, J. Kim, M. Wulff, J.J. van Thor, H. Ihee, *J. Am. Chem. Soc.* 134 (2012) 3145.
- [12] Y. Hoshihara, Y. Imamoto, M. Kataoka, F. Tokunaga, M. Terazima, *Biophys. J.* 94 (2008) 2187.
- [13] M.A. van der Horst, I.H. van Stokkum, W. Crielgaard, K.J. Hellingwerf, *FEBS Lett.* 497 (2001) 26.
- [14] W.D. Hoff, A. Xie, I.H.M. van Stokkum, X.J. Tang, J. Gural, A.R. Kroon, K.J. Hellingwerf, *Biochemistry* 38 (1999) 1009.
- [15] E.F. Chen, T. Gensch, A.B. Gross, J. Hendriks, K.J. Hellingwerf, D.S. Kliger, *Biochemistry* 42 (2003) 2062.
- [16] A. Losi, T. Gensch, M.A. van der Horst, K.J. Hellingwerf, S.E. Braslavsky, *Phys. Chem. Chem. Phys.* 7 (2005) 2229.
- [17] W.D. Hoff, I.H.M. van Stokkum, H.J. van Ramesdonk, M.E. van Brederode, A.M. Brouwer, J.C. Fitch, T.E. Meyer, R. van Grondelle, K.J. Hellingwerf, *Biophys. J.* 67 (1994) 1691.
- [18] K. Takeshita, Y. Imamoto, M. Kataoka, K. Mihara, F. Tokunaga, M. Terazima, *Biophys. J.* 83 (2002) 1567.
- [19] Y.O. Jung, J.H. Lee, J. Kim, M. Schmidt, K. Moffat, V. Srajer, H. Ihee, *Nat. Chem.* 5 (2013) 212.
- [20] J. Tenboer, S. Basu, N. Zatsepin, K. Pande, D. Milathianaki, M. Frank, M. Hunter, S. Boutet, G.J. Williams, J.E. Koglin, D. Oberthuer, M. Heymann, C. Kupitz, C. Conrad, J. Coe, S. Roy-Chowdhury, U. Weierstall, D. James, D.J. Wang, T. Grant, A. Barty, O. Yefanov, J. Scales, C. Gati, C. Seuring, V. Srajer, R. Henning, P. Schwander, R. Fromme, A. Ourmazd, K. Moffat, J.J. Van Thor, J.C.H. Spence, P. Fromme, H.N. Chapman, M. Schmidt, *Science* 346 (2014) 1242.
- [21] T.W. Kim, C. Yang, Y. Kim, J.G. Kim, J. Kim, Y.O. Jung, S. Jun, S.J. Lee, S. Park, I. Kosheleva, R. Henning, J.J. van Thor, H. Ihee, *Phys. Chem. Chem. Phys.* 18 (2016) 8911.
- [22] N.M. Derix, R.W. Wechselberger, M.A. van der Horst, K.J. Hellingwerf, R. Boelens, R. Kaptein, N.A.J. van Nuland, *Biochemistry* 42 (2003) 14501.
- [23] A.H. Xie, W.D. Hoff, A.R. Kroon, K.J. Hellingwerf, *Biochemistry* 35 (1996) 14671.
- [24] Y. Imamoto, K. Mihara, O. Hisatomi, M. Kataoka, F. Tokunaga, N. Bobjkova, K. Yoshihara, *J. Biol. Chem.* 272 (1997) 12905.
- [25] S. Anderson, S. Crosson, K. Moffat, *Acta Crystallogr. D Biol. Crystallogr.* 60 (2004) 1008.
- [26] S. Rajagopal, S. Anderson, V. Srajer, M. Schmidt, R. Pahl, K. Moffat, *Structure* 13 (2005) 55.
- [27] S. Devanathan, S. Lin, M.A. Cusanovich, N. Woodbury, G. Tollin, *Biophys. J.* 79 (2000) 2132.
- [28] B. Borucki, H. Otto, C.P. Joshi, C. Gasperi, M.A. Cusanovich, S. Devanathan, G. Tollin, M.P. Heyn, *Biochemistry* 42 (2003) 8780.
- [29] B. Borucki, S. Devanathan, H. Otto, M.A. Cusanovich, G. Tollin, M.P. Heyn, *Biochemistry* 41 (2002) 10026.
- [30] U.K. Genick, S. Devanathan, T.E. Meyer, I.L. Canestrelli, E. Williams, M.A. Cusanovich, G. Tollin, E.D. Getzoff, *Biochemistry* 36 (1997) 8.
- [31] J. Choi, C. Yang, J. Kim, H. Ihee, *J. Phys. Chem. B* 115 (2011) 3127.
- [32] C. Yang, J. Choi, H. Ihee, *Phys. Chem. Chem. Phys.* 17 (2015) 22571.
- [33] J.S. Khan, Y. Imamoto, M. Harigai, M. Kataoka, M. Terazima, *Biophys. J.* 90 (2006) 3686.
- [34] K. Takeshita, Y. Imamoto, M. Kataoka, F. Tokunaga, M. Terazima, *Biochemistry* 41 (2002) 3037.
- [35] J.S. Khan, Y. Imamoto, Y. Yamazaki, M. Kataoka, F. Tokunaga, M. Terazima, *Anal. Chem.* 77 (2005) 6625.
- [36] J. Hendriks, W.D. Hoff, W. Crielgaard, K.J. Hellingwerf, *J. Biol. Chem.* 274 (1999) 17655.